Catalysis Today xxx (2015) xxx–xxx

Contents lists available at ScienceDirect

Catalysis Today

journal homepage: www.elsevier.com/locate/cattod

Photocatalytic hydrophobic concrete coatings to combat air pollution

M. Faraldos[a,b,*], R. Kropp[a], M.A. Anderson[a,c], K. Sobolev[d]

[a] Water Science and Engineering Laboratory, University of Wisconsin-Madison, USA
[b] Instituto de Catálisis y Petroleoquímica, CSIC, Spain
[c] IMDEA Energia, Madrid, Spain
[d] University of Wisconsin-Milwaukee, USA

ARTICLE INFO

Article history:
Received 24 March 2015
Received in revised form 27 May 2015
Accepted 15 July 2015
Available online xxx

Keywords:
Concrete
Hydrophobic
Photocatalysis
Self-cleaning
Air pollution
NO_x
Siloxane

ABSTRACT

Several low cost, user-friendly photocatalytic surface coatings were applied to cementitious surfaces and tested as a remediation technique for transportation NO_x emissions and organic pollutants. All of the sols (aqueous suspensions of nanoparticles) coatings showed very high nitrogen oxide (NO) conversion (~90%) and Methylene Blue dye bleaching when applied to concrete surfaces, even when the coatings were extremely thin or diluted, independently on the deposition method (spraying or dip coating). A novel hydrophobic coating based on photocatalyst nanoparticles suspended in a siloxane sealant showed similar conversion at low NO concentrations but required a greater loading of TiO_2. At high NO concentrations the hydrophobic coating was less effective, even at greater TiO_2 loadings, suggesting that the adsorption is the rate limiting step in this conversion process. A threshold of 1% TiO_2 loading in hydrophilic coating and 5% in the case of hydrophobic was needed to obtain a quantitative NO_x conversion. A home-made TiO_2 sol showed lower NO_x photodegradation but a more homogeneous and bonded layer.

1. Introduction

Oxidative photocatalysis based on the semiconducting properties of titanium dioxide (TiO_2) has attracted enormous interest since it was discovered in 1972 [1,2]. However, it is only in the last decade that photocatalytically active materials have been applied to urban infrastructures [3]. The use of these photocatalysts can provide a wide range of beneficial properties to a surface, like self-cleaning [4,5], treatment of gas phase contamination in indoor and outdoor air environments [6–10], mainly with volatile organic compounds (VOCs), nitrous oxides (NOx), sulfur oxides (SO_x), sooty particles, and reactive oxidative species (ROSs) [11,12].

Application of photocatalytically active material affects the surface area and surface energy of a structure or component and has several implications beyond its photo-oxidative property. Surfaces can be made to be more or less hydrophobic; profoundly different charge and energy, which has implications on the adhesion of coatings and subsequent surface treatments.

Recent advances in measurement techniques and methods have allowed the researcher to probe the oxidative effect of these coatings at environmentally relevant conditions. Indoor air contamination removal requires understanding the behavior of the system at air concentrations across the range of parts per trillion ($ppt_{v/v}$) to potentially parts per thousand (v/v) [13–16]. Measurements of the concentration of given pollutants are more viable in a closed space, where the air environment is protected from the vagaries of wind direction and other weather, byproducts from reactions are contained, and the list of common contaminants is relatively fixed [4]. When these same photocatalytic materials are studied in outdoor environments a subtle shift in weather (wind speed, wind direction, atmospheric pressure, humidity, air pressure, etc.) can dramatically affect the contaminant load of the photocatalytic surface [17,18]. The number of potential contaminants is much higher, as outdoor air contamination comes from many sources (industrial, plant and animal sources, fires, dust, water surface aerosolization, etc.), each of which have different composition and concentration profiles. In addition to the greater number of potential contaminants, determining the relevant degradation pathway is more complicated, as byproducts are immediately diluted and confounding or competing reactions occur.

Nitrogen oxides (NO_x) are an important air-polluting agent with impacts on smog formation, ozone generation, and direct human health effects [19–21]. These compounds are produced during high temperature combustion, particularly in internal combustion engines in vehicles [22]. Recent research has shown that making

* Corresponding author at: Instituto de Catálisis y Petroleoquímica, CSIC, C/ Marie Curie, 2 L10. Madrid. Spain.
E-mail address: mfaraldos@icp.csic.es (M. Faraldos).

http://dx.doi.org/10.1016/j.cattod.2015.07.025
0920-5861/

roadways photoactive through the application of TiO_2 is a promising approach for solving the problems caused by NO_x. The gas phase contaminant nitrous oxides are oxidized to nitrate ions at the concrete interface due to heterogeneous photocatalytic oxidation (PCO). The products of the reaction are in the form of water-soluble nitrate compounds and so can be washed from the active concrete surface by rain [23]. NO_x is typically present at sub-ppm concentrations in highly polluted rural air and even high levels of conversion to nitrates represent a small nitrate load on local water systems.

The incorporation of relatively low concentrations of titanium dioxide (TiO_2) in concrete formulation [24] and the use of the sunlight for the chemical conversion of nitrogen oxides [25,7] have become this technology an interesting alternative for urban construction. In addition, a few studies have shown that nano-TiO_2 can accelerate the early-age hydration of Portland cement, improve compressive and flexural strengths, and enhance the abrasion resistance of concrete [26]. Self-cleaning and "de-polluting" photocatalytic concrete products are already being produced by several companies in Europe and Japan for use in the facades of buildings and in paving materials for roads [27–29].

Improving air quality by producing photoactive infrastructure will require application of photoactive material to very large areas. In order to prove this treatment technology to be economically viable the cost of application and maintenance should be balanced against the removal or conversion of pollutants and the economic benefit to the public. Some studies have employed concrete blocks prepared by mixing TiO_2 particles with cementitious materials [30,31]. The amount of TiO_2 in these samples is very high and most of the catalyst is in the internal structure, where light is unavailable to promote reactions. Furthermore, mechanical properties of concrete are adversely affected by increasing concentrations of TiO_2 [32]. Other laboratory experiments have employed double layer blocks [17] [33], with only the upper layer having the photocatalyst in relatively high proportions. This preparation, requiring two steps, would ultimately result in increased production costs and some technical inconveniences such as blockage of the porous structure in the concrete and delamination of the photoactive facade. It is important to consider application procedures that are cost effective and these applications should not result in inferior mechanical, physical and chemical characteristics of the concrete [34]. While many contributions in the literature have been addressed to the effect of inlet gas flow, initial pollutant concentration, relative humidity, and irradiance, on the efficiency of photocatalytic degradation rates [17,35], little effort has been expended on optimizing the photocatalyst used, the method of its application or the homogeneity of distribution when preparing photoactive surfaces on concrete. In this sense, taking into account that photocatalytic reactions occur only at an illuminated surface, so an effective, sprayable photocatalytic coating material would be ideal.

On the other hand, siloxane sealers are typically applied to the surface of concrete to reduce ingress of harmful chemicals by creating hydrophobic conditions in the near surface areas, which combined with photocatalytic properties, could originate a new generation of materials offering better performance than conventional TiO_2 products.

2. Experimental procedure

2.1. Preparation of photocatalysts

Several different types of nano-particulate materials based on TiO_2 were used in this study: P25 powder from Degussa Evonik [36] (coded P), PC105 (C), PC500 (D) powders and, S5-300A (A) and S5-300B (B) sols, from CrystalACTIV [37], and an acidic TiO_2 sol (T) that was prepared in the lab by hydrolysis of titanium isopropoxide in diluted nitric acid media under energetic stirring, the mix was kept stirring for days until peptization and afterwards was dialyzed [38,39]. In addition, a home-made acidic silica (SiO_2) sol [40], prepared by hydrolysis of tetraethylortosilicate (TEOS) in acidic aqueous media and continuous stirring until peptization, was used in hydrophilic mixtures of some of these materials. Besides, a polymethyl-hydrogen siloxane (85–100%) oil, PMHS (XIAMETER MHX-1107) from Dow Corning with a specific gravity of 0.997 (at 25 °C) and a viscosity of 30 cSt was used as hydrophobic agent [41–43].

One of the primary concerns when choosing the photoactive materials was particle size. The particles should be small enough to achieve a homogeneous distribution of titania nanoparticles over the surface of concrete blocks, not alter the esthetic, be transparent to translucent, have a high surface area, produce a continuous coating, but not be small enough to be a health concern.

The main physico-chemical properties of photocatalysts were determined: sols composition and titanium quantification were analyzed by using an inductively coupled plasma with optical emission spectrophotometer Perkin-Elmer 3300DV. The crystallite size was estimated by applying the Scherrer equation to X-Ray diffraction data (PANalytical X'Pert). Specific surface area was calculated by BET method from data of nitrogen adsorption isotherms (Micromeritics, ASAP 2420). The surface morphology was analyzed by scanning electron microscopy (Hitachi Tablet Microscope TM-1000).

2.2. Preparation of concrete/mortar samples

Two different construction material supports were employed: concrete blocks and cement tiles. Concrete blocks were fabricated using a mix of crushed limestone coarse aggregate, graded sand, ordinary Portland cement and water in 3.47:1.87:1.0:0.45 proportion, respectively. Water reducing admixture (WRA) and air entraining agent (AEA) were added as necessary to produce a slump of 7.5 cm (±2.5 cm) and an entrained air content of 6% (±1%) when tested to ASTM standards. The WRA was added to half of the water and added to the coarse and fine aggregates in a mechanical concrete mixer and mixed for 1 min to moisten the aggregate particles. The cement was then added to the mixer, followed by the remainder of the water and the AEA. The concrete was mixed for 3 min, allowed to rest for 5 min, and then mixed for an additional 3 min. The concrete was cast into 10 cm × 10 cm × 30 cm molds and demolded after 24 h. The specimens were then transferred into a 100% RH curing chamber for 28 days.

The cement tiles were made from Portland cement mortar (1:1 cement:sand mix at W/C = 0.35) and cast into 15 cm × 15 cm × 1 cm stainless steel molds. After casting, the tiles were cured for 28 days in water.

After curing, all the specimens were sliced into small sample coupons (10 cm × 5 cm × 1 cm) using a diamond saw.

2.3. Concrete coating

The photoactive coating has been applied by two different procedures, spray and dip coating. The spraying method was used for home-made sols in order to control and minimize the amount employed, when the commercial sols and suspensions were applied spray or dip coating were used, except in the case of hydrophobic suspensions that presented a high viscosity to produce the aerosol. In the case of layers deposited by spraying, the amount of sol was varied to obtain 200, 500 and 1000 nm of theoretical thickness (calculated as, volume = desired layer thickness * specimen length * specimen width).

Please cite this article in press as: M. Faraldos, et al., Photocatalytic hydrophobic concrete coatings to combat air pollution, Catal. Today (2015), http://dx.doi.org/10.1016/j.cattod.2015.07.025

Several inorganic semiconducting oxides (commercial P25 (P) in suspension, S5-300A (A), S5-300B (B), synthetized TiO_2 (T) sols) and some of them mixed with home-made SiO_2 sol at different relative proportions, 100:0, 75:25, 50:50, 25:75 and 0:100 were spray coated on the concrete specimen surface. Furthermore, cement tile samples were prepared by dipping the coupons into the commercial S5-300A (A) and S5-300B (B) sols of the TiO_2 particles. For each application, the tile was placed in the TiO_2 suspension for 10 s and then withdrawn and allowed to drip dry for 30 s. After coating, in both cases, spraying or dipping, the specimens were dried for 1 h at 50 °C. Three different series, depending on the concentration of aqueous commercial TiO_2 employed were coated: (i) 100% (A-20/B-18), (ii) 10% (A-2.0/B-1.8) and (iii) 1% (A-0.2/B-0.18). And two different coating thickness were prepared: one layer (A/B1) and three layers (A/B3), following the same described procedure for three consecutive times.

Two more series were prepared by dip coating to analyze the behavior of hydrophobic coatings, where commercial PC105 (C) and PC500 (D) TiO_2 powders, were suspended in siloxane superhydrophobic sealer at a dosage from 0.1 to 25%, although it was not possible to load more than 15% of PC500 (D) on siloxane due to the mixture became unworkable to be deposited by this procedure on cementitious surfaces.

The cement tiles specimens dip coated with the hydrophilic A and B commercial sols, and the C and D hydrophobic suspensions together with spray coated home-made TiO_2 sol were analyzed during NO photodegradation following the ISO 22197-1:2007 standard.

A block and a tile of cementitious materials without any coating were used as reference for all experiments using the same reaction conditions than samples.

Table 1 summarizes catalysts, coating procedures and samples codification.

2.4. Methylene Blue photodegradation

A qualitative evaluation of the photocatalytic degradation capacity was performed by depositing a drop of Methylene Blue (MB) dye solution (10^{-2} M MB) on the coated concrete samples. Photocatalytic activity was judged by measuring the reduction of stain area and the disappearance of color under illumination (10 W m^{-2} halogen light, no UV filter). The evolution of the stains with time was followed by photographs taken at different reaction times and further image histogram analysis using the software ImageJ64 1.35.

2.5. NOx photodegradation: FTIR detection

A scheme of the experimental design is represented in Fig. 1A. Two pieces of concrete block samples (10 cm × 5 cm × 1 cm) were located in a gas-tight borosilicate glass reactor surrounded by five 15 W fluorescent lamps, three Black Blue Light (BBL) and two daylight (DL) lamps. The reactor was attached to a 100 ppm NO and zero air gas cylinders, a gas mixer was used to generate the desired NO concentration at the inlet that was stablished at 90 ppm to assure an adequate FTIR detection during photo-oxidation evolution. A 1.2 L min^{-1} constant inlet flow of gas was passed through the reactor. A Harrick multi-pass FTIR sampling gas cell fitted to a Nicolet FTIR spectrometer was used for detection. An FTIR spectrum was recorded every 13 min throughout the 20–25 h of experimental duration in recirculating conditions. The system was allowed to equilibrate with the lights off for 10 h, illuminated for 5 h, and then allowed to re-equilibrate for 7 h. All the experiments were performed at room temperature (25 °C).

Table 1
Main coating characteristics, samples preparation and codification names, and test carried out for each sample.

Catalyst	TiO_2 (%)	Coating composition	Coating pH	Crystallite size (nm)	S_{BET} (m^2 g^{-1})	Coating method	No. layers	Thickness (nm)	Surface modificators	Support	Sample names	Performed tests
TEA	20	Ti sol	2–3	3.8	340	Spray	1	200 500 1000	SiO_2 sol	Concrete	T1-20	MB NO_x^{FTIR} NO_x^{ISO}
S5-300A	20	P,S,Ti sol	1	6.6	352	Spray Dip coating	1/3	1000 >2000	–	Concrete Cement	A1/3[a] 20-2.0-0.2[b]	MB NO_x^{ISO}
S5-300B	18	S,Ti sol	11	7.4	338	Spray Dip coating	1/3	1000 >2000	–	Concrete Cement	B1/3[a] 18-1.8-0.18[b]	MB NO_x^{ISO}
P25	99.5	Ti suspension	5.9	21.4	54	Spray	1	200 500 1000	SiO_2 sol	Concrete	P1-20	MB NO_x^{ISO}
PC 105	95	S, Ti suspension	6.0	19.4	79	Dip coating	1/3	>2000	Siloxane	Cement	C1-0.1-25	NO_x^{ISO}
PC 500	85	S, Ti suspension	6.3	8.7	359	Dip coating	1/3	>2000	Siloxane	Cement	D1-0.1-15	NO_x^{ISO}

[a] Depending on number of coated layers.
[b] Depending on TiO_2 concentration on sol/suspension coating.

Please cite this article in press as: M. Faraldos, et al., Photocatalytic hydrophobic concrete coatings to combat air pollution, Catal. Today (2015), http://dx.doi.org/10.1016/j.cattod.2015.07.025

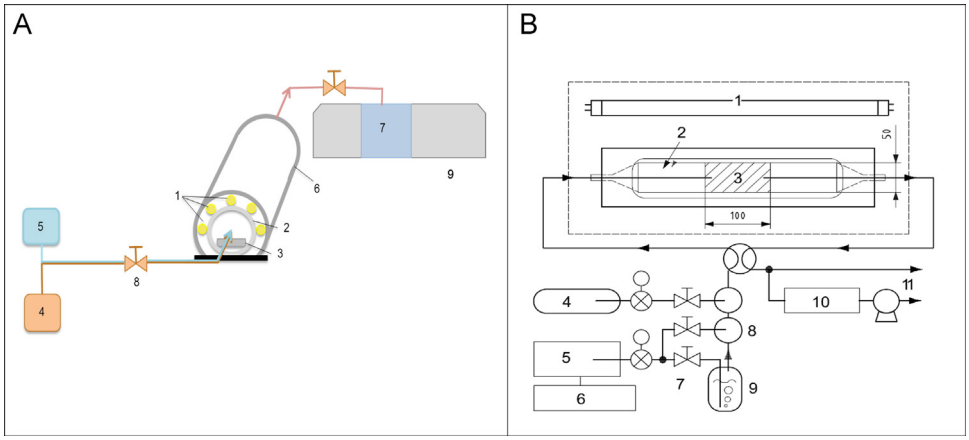

Fig. 1. Scheme of reaction system set up. (A) *FTIR detection*: 1. Light source, 2. Borosilicate reactor, 3. Sample, 4. Gas pollutant, 5. Zero air cylinder, 6. Aluminum foil, 7. Gas cell, 8. Gas mixer, 9. FTIR instrument. (B) *Chemiluminescence detection*: 1. Light source, 2. Optical window, 3. Test specimen, 4. Gas pollutant, 5. Air-purification, 6. Air compressor, 7. Mass-flow controllers, 8. Gas mixers, 9. Humidifier, 10. Analyzer, 11. Vent.

2.6. NOx photodegradation: chemiluminescence detection

A schematic diagram of the experimental setup is shown in Fig. 1B. The reaction chamber and all other components were designed according to the ISO 22197-1:2007 standard [44], however some reaction variables were modified for research purposes (NO inlet concentration and gas flow). The reaction chamber was made of non-absorbing plastic, covered by a borosilicate window and completely sealed to avoid loss of the NO gas–air mixture. A fan was used to spread out the gas mixture uniformly all over the chamber. A 150 W high-pressure mercury lamp was used as the light source that provided an irradiance of 10 W m^{-2}. A sparging column was used to humidify the zero air prior to mixing. The relative humidity was stablished at 50 ± 3% by a humidity controller. Gas from the 100 ppm NO cylinder was blended with the humidified zero air to meet the desired NO inlet concentration. The gas flow levels were kept constant between 1.4 and 1.5 L min^{-1}. All of the experiments were performed at room temperature (25 °C) and inlet NO concentration of 1.5 ppm and 15 ppm. An NO/NO_x Thermo Scientific Analyzer Model 42i was used to measure the NO concentration.

3. Results and discussion

3.1. Methylene Blue (MB) photodegradation

Methylene Blue (MB) testing provided different type of information; firstly, the spot area yielded some indication of the hydrophobicity of the coating, the higher hydrophilicity the wider area for the same deposited MB solution volume. Besides that lightening of the blue color could be related to photocatalytic oxidative behavior of the concrete or coated concrete samples.

The bleaching of MB spots was essayed on concrete samples spray-coated with home-made TiO_2 (T) sol, commercials TiO_2 P25 (P), S5-300A (A), S5-300B (B) and mixtures of some of these photocatalysts with lab-made SiO_2 sols (Table 1). The results (Fig. 2) showed that even references were able to whitening the MB spots, which highlights one of the difficulties when performing experiments on concrete specimens, where porosity and pore humidity/pH could cause hydrolysis in absence of light due to the basicity of concrete pore water [45,46], while in the silica sol coated could be originated by deeper adsorption of MB promoted by the hydrophilicity of acidic SiO_2 sol, joined to photochemical decoloration [47–49]. The quantification of spot area reduction and, specially, the calculated MB initial photodegradation rate (Table 2)

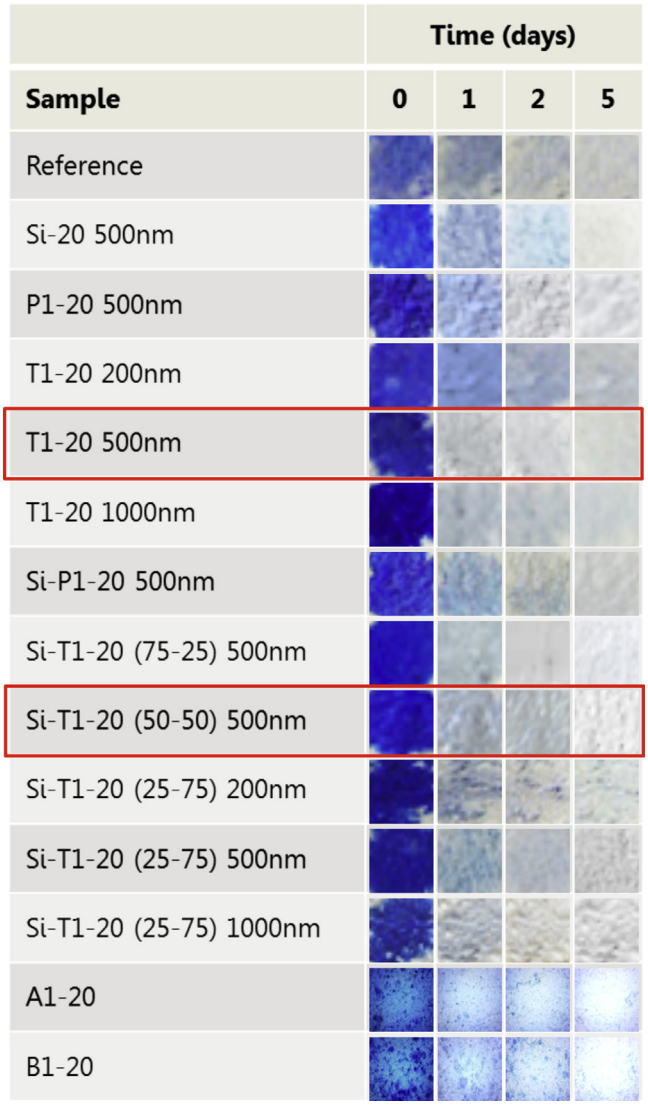

Fig. 2. MB bleaching over coated concrete samples.

Table 2
Estimation of MB photodegradation as spot area reduction and initial MB photodegradation as area decrease per time. (The faster MB photodegradation was obtained with samples marked in bold).

Sample	Coating composition (%)	Area (pixel)	Area shrinkage (%)	$r_{0,MB\ degradation}$ (pixel s^{-1})
Reference	0	500	40	3.6×10^{-4}
Si-20[a]	100	510	42	3.3×10^{-4}
T1-20[a]	**100**	**520**	**57**	$\mathbf{5.2 \times 10^{-4}}$
Si-T1-20[a]	75-25	450	50	5.0×10^{-4}
Si-T1-20[a]	**50-50**	**450**	**66**	$\mathbf{5.3 \times 10^{-4}}$
Si-T1-20[a]	25-75	650	44	5.0×10^{-4}
Si-P1-20[a]	50-50	750	44	4.8×10^{-4}

[a] Theoretical coated layer thickness: 500 nm. One layer was sprayed of TiO_2 20% concentrated sol or suspension.

pointed out the significant photocatalytic activity presented by the coated specimens that exhibited larger and faster decreases of stained area under halogen light activation. These results suggested that home-made TiO_2 sol coatings appear to increase the rate of MB conversion due to photocatalytic activity. Higher degradation rates were obtained for the concrete block samples with 500 nm thick films of home-made silica-titania sols (Si-T1-20, 50-50 proportion respectively) and 100% TiO_2 (T1-20) sol, while other silica-titania sols (Si-T1-20 75-25 and 25-75), silica sol-P25 titania (Si-P1-20) suspension (50-50) gave rise to slightly lower MB photoefficiency. The co-presence of SiO_2–TiO_2 looks to favor the photocatalytic degradation probably due to cooperation between higher adsorption associated to superficial Si–OH directly responsible of the enhancement of photocatalytic TiO_2 efficiency, since $^{\bullet}OH$ radicals have a greater probability to find a MB adsorbed molecule than an e^- to recombine. Under halogen light, the dark blue color of MB deposited on these samples completely disappeared after 120 h, even at shorter times for some of the studied coatings. This simple test could be a rapid method of preliminary estimating the potential photoactivity capacity of different coatings, but special care has to be taken to not extrapolate these findings to other organic pollutants photodegradation.

A selection of the coated surfaces was analyzed by SEM (scanning electron microscopy) and the images (Fig. 3) showed a very different layer adhesion, the home-made TiO_2 presented the most homogeneous and regular layer while the commercial A1-20 and B1-20 coatings had crashes and some pieces were peeled out. Furthermore, Si-20 concrete block coating presented a poor adhesion and a damaged surface with many cracks, while the presence of home-made SiO_2 in the lab prepared nanoparticulate TiO_2 coating seems to worsen the adhesion of the layer. In order to provide a satisfactory durability of coated cementitious surfaces, a homogeneous and well adhering layer should be achieved even at the expense of a small loss of photoactivity.

3.2. FTIR study: NO photodegradation

The FTIR study revealed the formation of no other detectable by-products than NO and NO_2 during long term NO photodegradation on selected home-made SiO_2 and TiO_2 coated concrete samples. The characteristic high resolution doublet peaks corresponding to both NO at 1960–1760 cm^{-1} and NO_2 at 1670–1540 cm^{-1} (Fig. 1, Supplementary Information) presented very different sensitivity (1:10 respectively) and were quantified by area integration. Approximately 8–10 h of concrete sample exposure to the inlet flow was required to reach a steady state. This is due to the adsorption of NO on the surface of the porous concrete [50]. It took longer to reach steady state when more porous concrete structure was available, because in these experiments the surfaces not exposed directly to light were not blocked to adsorption by any sealant, like usually

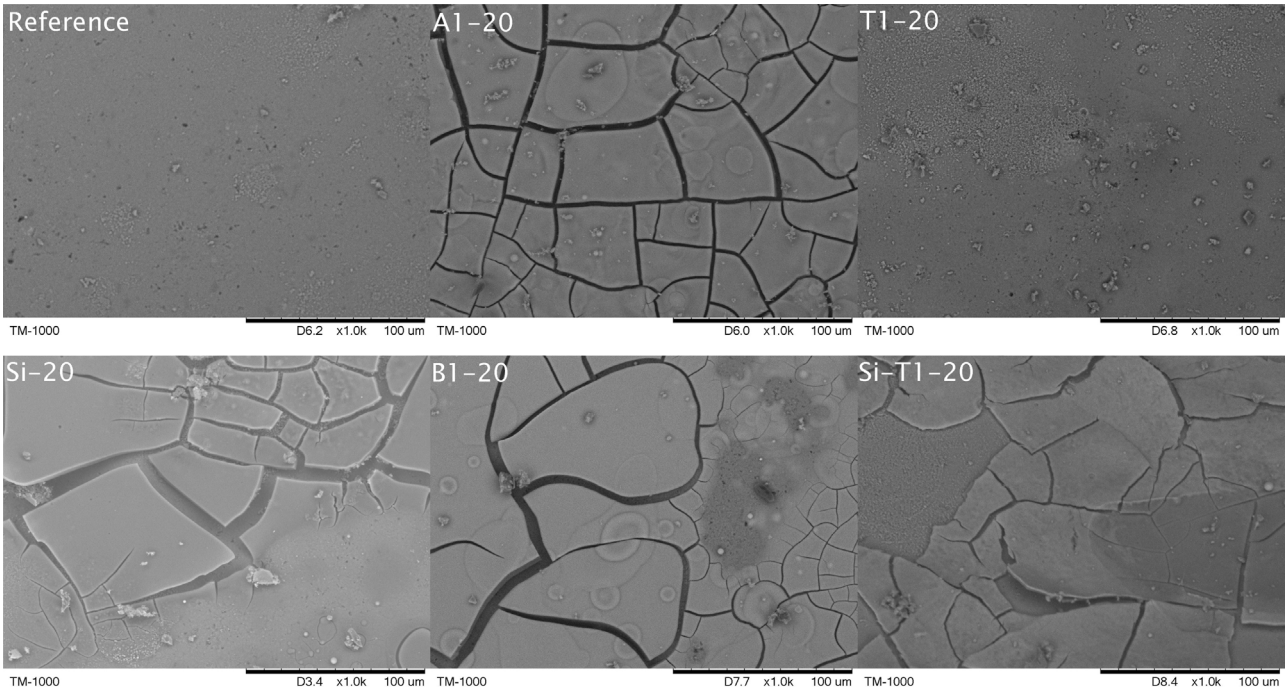

Fig. 3. SEM pictures of home-made and commercial TiO_2 sols coated on cementitious surfaces. Images of raw and home-made SiO_2 sol coated surfaces have been included as references.

Please cite this article in press as: M. Faraldos, et al., Photocatalytic hydrophobic concrete coatings to combat air pollution, Catal. Today (2015), http://dx.doi.org/10.1016/j.cattod.2015.07.025

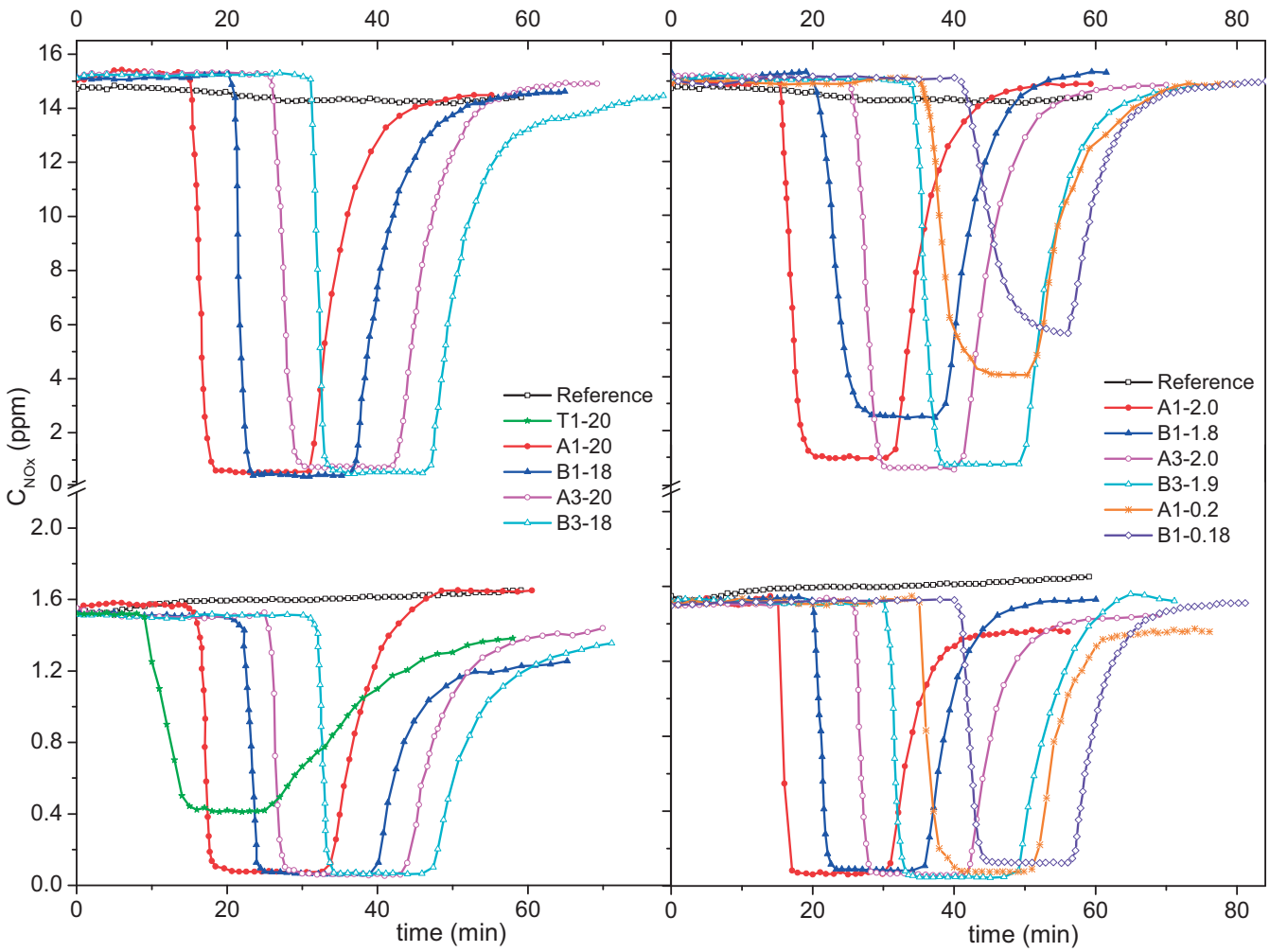

Fig. 4. Evolution of NOx concentration during photodegradation reaction. Effect of nature, concentration and number of layers of TiO_2 coating.

prescribed when normalized experiments are carried out. In this sense, it is likely that the highly porous concrete adsorbed not only NO but the in situ oxidation product, NO_2; moreover, coated samples had a higher degree of adsorption, probably due to the porous microstructure contribution of the coating layer [50] [51] or to the presence of functional groups with higher affinity for adsorbing NO and NO_2 [52]. In these conditions, the magnitude of the photocatalytic effect was not significantly enough to provoke a NO_x concentration decrease clearly detected by FTIR and assignable to photocatalytic degradation, worsened by the low sensitivity to NO.

Supplementary figure related to this article can be found, in the online version, at http://dx.doi.org/10.1016/j.cattod.2015.07.025

Some estimation of NO adsorbed, oxidation to NO_2 and, finally, NO and NO_x ($NO + NO_2$) disappearance, could be made by integration of NO and NO_2 double-peaks areas (Table 3) and the subsequent study of areas evolution with dark and irradiation times. The NO_2 peaks, corresponding to partial oxidation of NO fed, were larger for the Si-T1 50-50 and Si-T1 25-75, even T1-20, 500 nm thickness coated specimens that correspond with the higher NO conversion, however the presence of lower loading of TiO_2, like in Si-T1 75-25, gave rise to the maximum NO_x disappearance probably due to further oxidation of NO_2 to nitrate not detected because in the FTIR experiments carried out, a gas-cell was employed as sampling cell, and the concrete blocks could not be analyzed directly. The nitrate species formed could be trapped by cementitious materials reacting with the $CaCO_3$ present in to produce $Ca(NO_3)_2$ and CO_2 [27]. The experiments were maintained long term to assure the steady state indicating that the concrete surface reached the equilibrium.

3.3. NO photodegradation: chemiluminescence detection

The experimental apparatus was modified to attempt to isolate the effect of photocatalytic activity of the surface from the concrete adsorption. The use of thinner specimens and sealant application to all no photo-exposed surfaces tries to minimize the adsorption by the concrete bulk; in addition, the ISO 22197-1:2007 reaction chamber design reduces dead volumes minimizing adsorptive effects.

The application of TiO_2 coating and exposure to light resulted in a quick drop of the NO concentration within the chamber followed by a steady equilibrium state. The concentration of NO returned to the initial state after the lights were switched off. All cement tiles of A-20 and B-18 series (Fig. 4) demonstrated high conversion (95–97%), regardless of the initial NO concentration and independently of one or three TiO_2 layers applied. Equivalent NO photodegradation runs were carried out on mortar coated with 1:10 diluted TiO_2 sol: A-2.0 and B-1.8 series; and 1:100 diluted: A-0.20 and B-0.18 series, showing a complete NO conversion (higher than 92%) when the initial NO concentration was maintained at 1.5 ppm; however, when 15 ppm NO had to be removed by a very diluted coating (0.2% TiO_2) poorer conversions were

Table 3
Efficiency of home-made SiO_2–TiO_2 sols coated concrete. Estimation by FTIR spectra of NO adsorption, photo-oxidation to NO_2 and NO, NO_x disappearance.

Sample[a]	Reference	Si-20 (100-0)[b]	Ti-20 (0-100)[b]	Si-T1-20 (75-25)[b]	Si-T1-20 (50-50)[b]	Si-T1-20 (25-75)[b]
NO adsorption (%)[c]	3	4	5	7	5	4
NO to NO_2 oxidation (%)[d]	13	12	25	13	31	26
NO disappearance (%)[e]	15	14	30	20	35	29
NO_x disappearance (%)[f]	5	6	10	20	9	7

[a] Theoretical thickness coating 500 nm.
[b] Coating composition: proportion in percentage of Si-T1 sols.
[c] NO, ads (%) = $[(C_{NO,0} - C_{NO} - C_{NO_2})/C_{NO,0}] \times 100$.
[d] NO, ox (%) = $[C_{NO_2}/C_{NO,0}] \times 100$.
[e] NO, dis (%) = $[(C_{NO,0} - C_{NO})/C_{NO,0}] \times 100$.
[f] NOx,dis (%) = NO,ads + NO,dis − NO,ox.

Table 4
Efficiency and initial NOx photodegradation rate of hydrophilic TiO_2 coated tiles. Effect of TiO_2 sol, TiO_2 concentration, number of layers and NO initial concentration.

Sample	C_{TiO_2} coating (%)	Efficiency (%NO_x photodegraded)		$r_{0,NOx}$ ($mL\,L^{-1}\,min^{-1}$)	R^2	$r_{0,NOx}$ ($mL\,L^{-1}\,min^{-1}$)	R^2
		1.5 ppm	15 ppm	$C_{0,NO}$ = 1.5 ppm		$C_{0,NO}$ = 15 ppm	
Reference	0	26	8	0.045	0.975	0.014	0.955
T1-20	20	74	–	0.196	0.997	–	–
A1-20	20	95	96	0.417	0.934	6.161	0.973
B1-18	18	96	97	0.178	0.950	4.721	0.829
A3-20	20	96	95	0.714	0.975	4.983	0.978
B3-18	18	96	97	0.161	0.953	7.984	0.995
A1-2.0	2	96	93	0.453	0.893	4.723	0.993
B1-1.8	1.8	95	83	0.645	0.989	2.603	0.988
A3-2.0	2	96	96	0.860	0.963	4.572	0.993
B3-1.8	1.8	97	95	0.804	0.950	4.811	0.976
A1-0.2	0.2	95	73	0.466	0.953	1.280	0.947
B1-0.18	0.18	92	63	0.530	0.990	1.265	0.991

reached (63–73%, Table 4). These data suggest that even extremely thin or diluted layers of photocatalyst on the concrete surface could be enough to promote self-cleaning properties for building surfaces.

Meanwhile the behavior of the home-made TiO_2 spray coated concrete block, T1-20, presented an appreciable NOx photocatalytic conversion although lower than commercial photocatalysts layers. An interesting residual photoactivity was conserved even when illumination was switched off what could be related with longer lifetime of photogenerated active species in the case home-made TiO_2 coated cementitious specimens. Furthermore, the SEM pictures (Fig. 3) pointed out a more homogeneous and bonded layer than presented by commercial sols. Both characteristics make the T1-20 coating a very interesting alternative to combat air pollution.

The little effect on NO photodegradation efficiency of TiO_2 sol applied to the concrete tile surface could be related to large agglomerations of particles likely formed at high TiO_2 concentrations. Thus, some of the titania may have been inaccessible to NO gas or shielded from illumination. The same phenomenon could explain the behavior of tiles coated with three layers, where the first layer is too obscured to increase photoactivity. These results demonstrate that photocatalytic conversion was possible across a wide range of NO concentrations even on tile surfaces with low TiO_2 loading. Considering the usual values of NO concentration in the urban atmosphere could be assumed that using a diluted TiO_2 coating was enough to reduce the level of NO pollutant in the air.

When the initial NO_x photodegradation rates were compared (Table 4), series A coated cement tiles showed a similar value independently of TiO_2 sol dilution, while the sequential layer deposition accelerated the initial NO_x photodegradation. Contrarily series B was not affected by number of layers but the lower TiO_2 deposited the faster initial NO_x abatement, probably due to a more open-structure, more available to pollutants and with higher photo-exposed surface. The home-made TiO_2 showed an initial rate comparable to series B. In all cases, the reaction was speeding up when more concentrated NO was fed.

3.4. The effect of siloxane-based hydrophobic sealer on NOx photodegradation

The photoactivity of commercial PC105 TiO_2 powders (series C1-y cement tiles) on NO_x degradation was tested in siloxane hydrophobic sealer at TiO_2 dosage from 0.1 to 25 wt% by mass of sealer. As observed in Fig. 5A, for coatings with loading of PC105 TiO_2 (C) higher than 5%, C1-5 to C1-25 samples, the conversion of 1.5 ppm NO was almost constant (i.e. about 90%), while more diluted coatings, C1-0.1 and C1-1, presented conversions under 50%. Therefore, 5% of PC-105 (C) loading could be considered a threshold coating level to obtain a hydrophobic photoactive layer for NOx degradation. This is probably due to the siloxane blocks the pores in the titania particles, inhibiting NO_x adsorption and reducing the number of available active sites to those on the surface. Moreover the originated nitrates would be deposited in the hydrophobic tile surface, the inner diffusion through porous concrete structure and further reaction with calcium carbonate [27] should be disabled what could contribute to diminish the photocatalytic activity due to a secondary fouling effect.

This required loading value is greater than that found in coatings without siloxane, where concentrations of 2% produced a complete NO_x conversion and even around 0.2% showed a significant NO_x photodegradation, therefore hydrophilic loadings higher than 1% could not suppose any improvement in the NO_x abatement.

When 15 ppm NO concentration was fed into the reactor, NO_x conversion was maintained under only 40% independently of the PC105 (C) loading. As the amount of photocatalytic activity varies linearly with catalyst mass (Fig. 5A), this suggests that adsorption of NO on the surface was the rate limiting factor.

For the hydrophobic mixture of siloxane and PC500TiO_2 (D) coated cement tiles series the reduction efficiency at low NO inlet concentration (1.5 ppm) was practically 100% (Fig. 5B). In addition,

Please cite this article in press as: M. Faraldos, et al., Photocatalytic hydrophobic concrete coatings to combat air pollution, Catal. Today (2015), http://dx.doi.org/10.1016/j.cattod.2015.07.025

Table 5
Efficiency and initial NOx photodegradation rate of hydrophobic TiO_2 coated tiles. Effect of TiO_2 coating and NO initial concentrations.

Sample code	C_{TiO_2} coating (%)	Efficiency (%NO_x photodegraded)		$r_{0,NOx}$ (mL L^{-1} min^{-1})	R^2	$r_{0,NOx}$ (mL L^{-1} min^{-1})	R^2
		1.5 ppm	15 ppm	$C_{0,NO}$ = 1.5 ppm		$C_{0,NO}$ = 15 ppm	
C1-0.1	0.1	25	2	0.068	0.958	0.080	0.973
C1-1	1	48	2	0.235	0.992	0.085	0.979
C1-5	5	93	20	0.193	0.994	0.325	0.980
C1-10	10	87	32	0.426	0.979	0.652	0.987
C1-15	15	94	33	0.456	0.987	0.633	0.994
C1-20	20	95	39	0.300	0.996	1.399	0.975
C1-25	25	96	29	0.754	0.996	0.430	0.991
D1-0.1	0.1	90	3	0.040	0.992	0.099	0.988
D1-1	1	91	10	0.258	0.993	0.214	0.983
D1-5	5	99	44	0.531	0.993	0.989	0.990
D1-10	10	100	45	1.323	0.984	0.913	0.989
D1-15	15	100	67	0.593	0.986	1.375	0.992

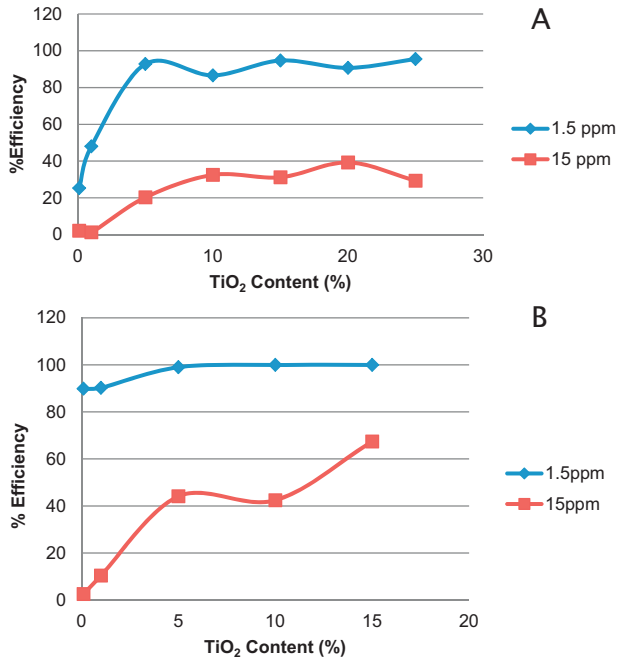

Fig. 5. Efficiency of NOx reduction on hydrophobic C1-y (A) and D1-y (B) TiO_2–siloxane coating series.

the NO_x elimination at more concentrated NO feed (15 ppm) kept increasing with photocatalyst loading, as a confirmation of the previously suggested that considers the adsorption of NO on the coated cement tile surface as a highlight limiting factor for photodegradation processes.

In parallel to the observed for series C tiles, a threshold of 5% TiO_2 loading, D1-1, looks necessary to completely photodegrade NO_x, but in series D tiles, higher efficiencies were always reached even for very light TiO_2 loadings, D1-0.1 to D1-5 (Fig. 5B). Therefore, PC500 (D) based TiO_2 result in a higher NO_x abatement than PC105 (C) based coating tiles at the same conditions. The higher efficiency showed by PC500 (D) hydrophobic coating could be due to the higher surface area capable to adsorb more NOx to be photodegraded, but, at the same time shows a lower particle size (Table 1) that could be related with a higher photo-exposed surface capable to produce more •OH radicals and extend the photoinduced reaction and the photodegradation rate as presented in Table 5.

4. Conclusions

Simple spraying or dip coating methods have been used to produce pollution remediating concrete. Photocatalytic coatings of TiO_2 nanoparticles and mixtures of SiO_2–TiO_2 sols proved to be highly effective at treating NO pollution and dye bleaching when applied to a concrete surface. High conversion of gas phase NO_x to surface bound nitrate species can have large effects on air pollution including smog and ozone. Using simple and inexpensive application methods and targeting application to the road surface near internal combustion vehicle sources can decrease the cost of adoption. Furthermore, preliminary testing of these coatings has shown improvements to mechanical properties of the concrete surface (in progress), giving the coatings dual purpose and worthy of further study. We are therefore continuing to pursue this line of investigation.

Hydrophobic photoactive nanoparticle coatings based on TiO_2 and siloxane sealant have demonstrated excellent ability to convert NO gas when applied to concrete surfaces. The average concentration of NO in polluted cities is approximately 0.01 ppm (10 ppb), much lower than our testing. Hydrophobic PC105 (C) and PC500 (D) TiO_2 coated cement tiles, with loadings above 5%, considered a threshold, exhibited 90% reduction of diluted NO pollutant, although improved efficiency was presented by series D, showing that these materials can perform well in even highly polluted areas or near pollution sources. When challenged by particularly high NO concentrations thicker coatings were required for adequate conversion.

During NO_x photocatalytic conversion on concrete hydrophilic surfaces, 1% of commercial studied TiO_2 content was enough to achieve a quantitative NO_x photodegradation. While the produced nitrates can be dispersed on concrete porosity to undergo further reaction with the calcium carbonate mostly present in the cement composition, to form calcium nitrate; when the photo-oxidation reaction happens on concrete hydrophobic surfaces, the nitrates could act as fouling to provoke a detrimental effect in photocatalytic efficiency.

FTIR analysis should be preferably applied to surface bonding species better than gases detection, because the sensitivity, in the case of NO and NO_2, was not competitive when compared to chemiluminescence detector, more selective and sensitive. In spite of that, feeding a more concentrated NO made possible to address this study.

Dye whitening photocatalytically induced is an adequate preliminary study to know the photoactivity showed by a surface, as could be observed in this case, notwithstanding, attempts to extrapolate MB photodegradation results to other pollutants photocatalytic abatement not always was possible, in this sense, the quantification of photocatalytic reaction extension could not be

Please cite this article in press as: M. Faraldos, et al., Photocatalytic hydrophobic concrete coatings to combat air pollution, Catal. Today (2015), http://dx.doi.org/10.1016/j.cattod.2015.07.025

inferred because it depends on pollutants and the different interaction with the surface.

In order to apply this technology to real life the durability study of the coating is a very important factor; as verified by SEM images, obtaining homogeneous and bonded layers of photocatalyst is not an easy question and home-made TiO_2 (T) sol became an interesting alternative due to the high NO_x conversion, MB bleaching and layer adhesion showed.

Acknowledgements

The first author gratefully acknowledges financial support from Spanish Plan Nacional I+D+i: scientists' mobility Program (ref. PR2009-0092) and project CTM2010-14883/TECNO. The authors acknowledge the financial support from UW Foundation Intercampus Research Grant and Emeni-ECO Ltd. Thanks to University of Wisconsin-Madison and University of Wisconsin-Milwaukee for the use of research facilities. Discussions and experimental setup with Dr. Isabel Tejedor at the University of Wisconsin-Madison and Dr. Andrey Sklyarov at the University of Wisconsin-Milwaukee are appreciated.

References

[1] A. Fujishima, K. Honda, Nature 238 (1972) 37.
[2] A. Mills, S. Le Hunte, J. Photochem. Photobiol. A: Chem. 108 (1997) 1–35.
[3] F. Pacheco-Torgal, S. Jalali, Constr. Build. Mater. 25 (2011) 582–590.
[4] A.Z.M. Rus, S.R. Mohid, S. Nurulsaidatulsyida, N. Marsi, Adv. Mater. Sci. Eng. (2013), http://dx.doi.org/10.1155/2013/486253, Article ID 486253, 9 p.
[5] J. Wanga, C.H. Lua, J.R. Xiong, Appl. Surf. Sci. 298 (2014) 19–25, http://dx.doi.org/10.1016/j.apsusc.2013.12.171
[6] J.S. Zhang, J.S. Zhang, Q. Chen, X. Yang, ASHRAE Trans. 108 (1) (2002) 162–174.
[7] J. Zhao, X. Yang, Build. Environ. 38 (2003) 645–654.
[8] J. Chen, S.-c. Kou, C.-s. Poon, Build. Environ. 46 (2011) 1827–1833.
[9] R.K. Nath, M.F.M. Zain, A.A.H. Kadhum, J. Appl. Sci. Res. 8 (8) (2012) 4147–4155.
[10] J. Schneider, M. Matsuoka, M. Takeuchi, J. Zhang, Y. Horiuchi, M. Anpo, D.W. Bahnemann, Chem. Rev. 114 (2014) 9919–9986, http://dx.doi.org/10.1021/cr5001892
[11] M.R. Hoffman, S.T. Martin, W. Choi, D.W. Bahnemann, Chem. Rev. 95 (1) (1995) 69–96.
[12] S. Devahasdin, C. Fan Jr., K. Li, D.H. Chen, J. Photochem. Photobiol. A: Chem. 156 (2003) 161–170.
[13] Air Quality in Europe, EEA Report 5, European Environment Agency, 2014.
[14] H. Minoura, A. Ito, Atmos. Environ. 44 (2010) 23–29.
[15] The Council of the European Union, EU Council Directive 1999/30/EC, Relating to Limit Values for Sulphur Dioxide, Nitrogen Dioxide and Oxides of Nitrogen, Particulate Matter and Lead in Ambient Air, 1999.
[16] M.M. Ballari, Q.L. Yu, H.J.H. Brouwers, Catal. Today 161 (2011) 175–180.
[17] M.M. Ballari, M. Hunger, G. Hüskena, H.J.H. Brouwers, Catal. Today 151 (2010) 71–76.
[18] S. Shen, M. Burton, B. Jobson, L. Haselbach, Constr. Build. Mater. 35 (2012) 874–883.
[19] D.L. Mauzerall, X. Wang, Atmos. Environ. 38 (26) (2004) 4383–4402.
[20] I.Y.R. Adamson, H. Prieditis, R. Vincent, Toxicol. Appl. Pharmacol. 157 (1999) 43–50.
[21] C.A. Pope III, D.W. Dockery, J. Air Waste Manage. Assoc. 56 (2006) 709–742.
[22] G. Hüsken, M. Hunger, H.J.H. Brouwers, Build. Environ. 44 (2009) 2463–2474.
[23] J.S. Dalton, P.A. Janes, N.G. Jones, J.A. Nicholson, K.R. Hallam, G.C. Allen, Environ. Pollut. 120 (2002) 415–422.
[24] C.-S. Yang, Y.-J. Wang, M.-S. Shih, Y.-T. Chang, C.-C. Hon, Appl. Catal. A: Gen. 364 (2009) 182–190.
[25] J.M. Herrmann, L. Péruchon, E. Puzenat, C. Guillard, in: P. Baglioni, L. Cassar (Eds.), Proceedings International RILEM Symposium on Photocatalysis, Environment and Construction Materials, Florence, Italy, October 8–9, 2007, RILEM Publications, Bagneux, 2007.
[26] I. Flores, L.M. Torres-Martinez, E.L. Cuellar, P.L. Valdez, E. Zarazua, Transp. Res. Rec.: J. Transp. Res. Board 2141 (2010) 10–14.
[27] Picada Project, www.picada-project.com
[28] Italcementi, www.italcementigroup.com or www.fym.es
[29] J. Chen, C.S. Poon, Build. Environ. 44 (2009) 1899–1906.
[30] M.M. Ballari, M. Hunger, G. Hüsken, H.J.H. Brouwers, Appl. Catal. B: Environ. 95 (2010) 245–254.
[31] M.M. Hassan, H. Dylla, L.N. Mohammad, T. Rupnow, Transportation Research Board 89th Annual Meeting, Washington, DC, January 11–15, 2010.
[32] J.F. Muñoz, R.C. Meininger, J. Youtcheff, Transp. Res. Rec.: J. Transp. Res. Board 2142 (2010) 34–41.
[33] H. Dylla, M.M. Hassan, L.N. Mohammad, T. Rupnow, E. Wright, Transp. Res. Rec.: J. Transp. Res. Board 2164 (2010) 46–51.
[34] P. Van den Heede, N. De Belie, Cem. Concr. Compos. 34 (2012) 431–442.
[35] A. Maury Ramirez, K. Demeestere, N. De Belie, T. Mäntylä, E. Levänen, Build. Environ. 45 (2010) 832–838.
[36] www.corporate.evonik.com
[37] www.crystalglobal.com
[38] D.H. Kim, M.A. Anderson, W.A. Zeltner, J. Environ. Eng. 121 (8) (1995) 590–594.
[39] http://www.marc-tech.com/Site/colloids.html
[40] M.A. Anderson, W.A. Zeltner, C.M. Merritt, Green technology for the 21st century: ceramic membranes, MRS Proc. 368 (1994) 377, http://dx.doi.org/10.1557/PROC-368-377
[41] K. Sobolev, V. Batrakov, ASCE J. Mater. Civil Eng. 19 (10) (2007) 809–819.
[42] K. Sobolev, V.G. Batrakov, ConcreteLife'09: 2nd International RILEM Workshop on Concrete Durability and Service Life Planning, Haifa, Israel, 2009.
[43] K. Sobolev, H. Tabatabai, J. Zhao, I. Flores-Vivian, R. Rivero, S. Muzenski, M.G. Oliva, R. Rauf, Superhydrophobic Engineered Cementitious Composites for Highway Bridge Applications: Phase I, National Center for Freight & Infrastructure Research & Education, CFIRE 04-09, University of Wisconsin-Milwaukee, University of Wisconsin-Madison, 2013, May.
[44] ISO 22197-1:2007 – Fine ceramics (advanced ceramics, advanced technical ceramics), Test method for air-purification performance of semiconducting photocatalytic materials – Part 1: Removal of nitric oxide.
[45] T. Yuranova, V. Sarria, W. Jardim, J. Rengifo, C. Pulgarin, G. Trabesinger, J. Kiwi, J. Photochem. Photobiol. A: Chem. 188 (2007) 334–341.
[46] J. Tschirch, R. Dillert, D. Bahnemann, B. Proft, A. Biedermann, B. Goer, Res. Chem. Intermed. 34 (4) (2008) 381–392.
[47] A. Houas, H. Lachheb, M. Ksibi, E. Elaloui, C. Guillard, J.M. Herrmann, Appl. Catal. B: Environ. 31 (2001) 145–157.
[48] D.H. Lee, S.Y. Choi, Met. Mater. Int. 10 (4) (2004) 357–360.
[49] C. Mendoza, A. Valle, M. Castellote, A. Bahamonde, M. Faraldos, Appl. Catal. B: Environ. 178 (2015) 155–164, http://dx.doi.org/10.1016/j.apcatb.2014.09.079
[50] J. Zhang, J.S. Zhang, Q. Chen, X. Yang, ASHRAE Trans. 108 (1) (2002) 162.
[51] J. Chen, C.S. Poon, Environ. Sci. Technol. 43 (2009) 8948–8952.
[52] A. Folli, S.B. Campbell, J.A. Anderson, D.E. Macphee, J. Photochem. Photobiol. A: Chem. 220 (2011) 85–93.

Please cite this article in press as: M. Faraldos, et al., Photocatalytic hydrophobic concrete coatings to combat air pollution, Catal. Today (2015), http://dx.doi.org/10.1016/j.cattod.2015.07.025